Neurotoxicity Research (2019) 36:66–80
https://doi.org/10.1007/s12640-019-00016-y

ORIGINAL ARTICLE

Mn-Induced Neurocytes Injury and Autophagy Dysfunction in Alpha-Synuclein Wild-Type and Knock-Out Mice: Highlighting the Role of Alpha-Synuclein

Dong-Ying Yan[1] · Chang Liu[1] · Xuan Tan[1] · Zhuo Ma[1] · Can Wang[1] · Yu Deng[1] · Wei Liu[1] · Zhao-Fa Xu[1] · Bin Xu[1]

Received: 18 October 2018 / Revised: 29 December 2018 / Accepted: 12 February 2019 / Published online: 22 February 2019

Abstract

Overexposure to manganese (Mn) is an important environmental risk factor for Parkinsonian-like symptoms referred to as manganism. Alpha-synuclein (α-Syn) oligomerization is a major cause in Mn-induced neurotoxicity. Autophagy, as an adjust response to control intracellular protein homeostasis, is involved in the degradation of α-Syn monomers or oligomers. Furthermore, autophagy dysregulation is also related to development of neurodegenerative disorders. Hence, we speculated that there was an interaction effect between α-Syn oligomerization and autophagy upon Mn exposure. In this study, we applied α-Syn gene knockout mice (α-Syn$^{-/-}$) and wild-type mice (α-Syn$^{+/+}$) treated with three different concentrations of $MnCl_2$ (50, 100, and 200 μmol/kg) to elucidate the physiological role of α-Syn in Mn-induced autophagy dysregulation and neurocytes injury. We found that activation of chaperone-mediated autophagy (CMA) pathway by Mn was independent of α-Syn. Additionally, α-Syn could ameliorate excessive autophagy induced by high dose Mn (200 μmol/kg). Next, we used 5 mg/kg Rapamycin (Rap) or 3-methyladenine (3-MA) to regulate autophagy. The study revealed that autophagy is involved in Mn-induced α-Syn oligomerization and neurocytes injury. Taken together, these findings indicated that α-Syn oligomerization might be the major responsible for the Mn-induced autophagy dysregulation and neurocytes injury.

Keywords Manganese · Alpha-synuclein oligomerization · Autophagy · Apoptosis · Neurotoxicity

Abbreviations

Mn	Manganese
PD	Parkinson's disease
BBB	Blood-brain barrier
CNS	Central nervous system
α-Syn	Alpha-synuclein
CMA	Chaperone-mediated autophagy
Rap	Rapamycin
3-MA	3-Methyladenine
I.P.	Intraperitoneal
S.C.	Subcutaneously
MDC	Monodansylcadaverine

Electronic supplementary material The online version of this article (https://doi.org/10.1007/s12640-019-00016-y) contains supplementary material, which is available to authorized users.

✉ Bin Xu
bxu10@cmu.edu.cn

[1] Department of Environmental Health, School of Public Health, China Medical University, No. 77 Puhe Road, Shenyang North New Area, Shenyang, Liaoning 110122, People's Republic of China

Introduction

Manganese (Mn), as one of necessary trace elements, is important for sustaining normal physical function (O'Neal and Zheng 2015). However, excessive and chronic exposure to Mn can cause neurotoxicity resulting in neurodegenerative disorder, referred to as manganism, characterized by Parkinsonian-like symptoms (Chen et al. 2015). Mn has been implicated in neurodegeneration due to its role as a neurotoxicant upon excessive exposure (Horning et al. 2015). Epidemiological studies have reported that a high level in occupational or environmental setting of Mn is tightly associated with increased risk for neurodegenerative disease (O'Neal and Zheng 2015). Therefore, Mn exposure becomes an important environmental risk for this disorder with Parkinsonian-like symptoms.

Previous studies on the mechanism of Mn neurotoxicity have mainly focused on mitochondrial dysfunction, oxidative stress,

apoptosis, alteration of neurotransmitter metabolism, and calcium homeostasis (O'Neal and Zheng 2015). Nevertheless, emerging evidence indicates that alpha-synuclein (α-Syn) oligomerization is a major culprit for Mn-induced neurotoxicity (Xu et al. 2014a). α-Syn, as a chaperon protein with 140 amino acids, is widely expressed in neural tissue where it predominantly localizes to the presynaptic terminal. It can play important roles in the regulation of synaptic plasticity, vesicle transport, and dopaminergic neurotransmission (Benskey et al. 2016). Under some pathogenic conditions (oxidative stress and exposed to metal, etc.), α-Syn can spontaneously develop into stable oligomers themselves eliciting adverse events, including perturbing cellular proteostasis, damaging membrane structure, and inducing cell death (Gonzalez-Horta 2015). However, the exact mechanism of α-Syn monomers or oligomers in autophagy induction is still limited.

Autophagy is a conserved degradation and recycling cellular process essential for maintaining homeostasis at low basal levels, which is grouped microautophagy, macroautophagy, and chaperone-mediated autophagy (CMA). Emerging evidence indicate that the degradation of misfolded/unfolded proteins depend on both macroautophagy and CMA pathways (Ciechanover and Kwon 2015). Autophagy functions as an essential cytoprotective response to varying insults (misfolded/aggregated proteins and damaged organelles). However, autophagy dysregulation (excessive activation or inhibition) are connected with the development of neurodegenerative disorders (Zhang et al. 2016). Although several studies have reported that Mn could induce autophagy dysregulation (Yuan et al. 2016; Zhang et al. 2013), little data exist on α-Syn oligomerization involved in Mn-induced autophagy dysregulation.

Based on above findings, we speculate that α-Syn monomer may play protective role in ameliorating Mn-induced excess autophagy and neurocytes injury. Conversely, α-Syn oligomers exacerbate Mn-induced neurocytes injury, and autophagy also tightly involves in Mn-induced α-Syn oligomerization and neurotoxicity. Therefore, in this study, we explored the important effect of α-Syn on Mn-induced autophagy and apoptosis by α-Syn gene knockout (α-Syn$^{-/-}$) mice vs. wild-type (α-Syn$^{+/+}$) mice. Furthermore, rapamycin (Rap) and 3-methyladenine (3-MA), autophagy regulators, were introduced into our current study to confirm that there was a relationship between α-Syn oligomerization and Mn-induced autophagy dysregulation.

Materials and Methods

Materials

Manganese (II) chloride tetrahydrate and propidium iodide (PI) were obtained from Sigma Chemical Co. (St. Louis, MO, USA). Rapamycin (Cat #: HY-10219) and 3-methyladenine (Cat #: HY-19312) were from MedChem Express (USA). Annexin V-FITC/PI reagent kit was purchased from Nanjing KeyGen Biotech. Co. Ltd. (Cat No: KGA 106; China). *PrimeScript*® RT Enzyme Mix I and SYBR® Premix Ex *Taq*™ II kits were from TaKaRa Biotech. Co. Ltd. Mouse α-Syn, HSC70, p62 monoclonal primary antibody and rabbit Beclin1, LC3B, and Lamp2A polyclonal primary antibody were purchased from Abcam Ltd. (Hong Kong). Horseradish peroxidase (HRP) conjugated anti-rabbit secondary antibody and HRP conjugated anti-mouse secondary antibody were purchased from Abcam. Other chemicals of analytical grade applied in current study were obtained from local chemical suppliers.

Animals and Treatments

Homozygous α-Syn gene knockout (α-Syn$^{-/-}$) male mice were purchased from Jackson Laboratory (B6; 129X1-Snca^{tmlRosl}, stock #003692, Bar Harbor, MA). According to the previous reports, a stable breeding colony could be expanded and maintained by heterozygous offsprings crossed (Ding et al. 2016). In our study, α-Syn$^{-/-}$ male mice were crossed with the wild-type female mice (C57/BI6J) to yield heterozygous mice (F1). Then heterozygous offsprings (F2 × F2 and F3 × F3…) crosses were conducted to maintain a stable breeding colony. As shown in Fig. 1, animal genotype was confirmed by PCR amplification of genomic DNA set for *α-Syn* gene. Ten-week-old homozygous α-Syn$^{-/-}$ and α-Syn$^{+/+}$ mice (25 ± 5 g) (female:male = 1:1) from identical offspring generation of F5 heterozygotes were carried out in experiments (Fig. 1a, b).

Animal treatment and care were in accordance with the National Institutes of Health Guidelines for the Care and Use of Laboratory Animals and approved by the Animal Ethical Committee of China Medical University. This study was divided into two parts. For the first part, we set up each four groups of α-Syn$^{+/+}$ and α-Syn$^{-/-}$ mice (10-week-old) (n = 10 per group) (female:male = 1:1): control (NaCl), three different dosage of $MnCl_2$ (50, 100, and 200 μmol/kg) groups. The manner of treatment was conducted by intraperitoneal (i.p.) injection for five consecutive days every week (Krishna et al. 2014). During the exposure period, the mice were periodically subjected to behavioral tests every 2 weeks and at the sixth week we observed obvious behavioral impairment, which indicated that the animals model of manganism were successfully established and relevant indicators were able to collect for detection. For the second part, we used Rap and 3-MA to pretreat 200 μmol/kg Mn-treated α-Syn$^{+/+}$ mice. These mice were randomly divided into six groups (10-week-old) (n = 10 per group) (female:male = 1:1): control groups (NaCl control, Rap control, and 3-MA control), 200 μmol/kg $MnCl_2$-treated group, and Rap or 3-MA

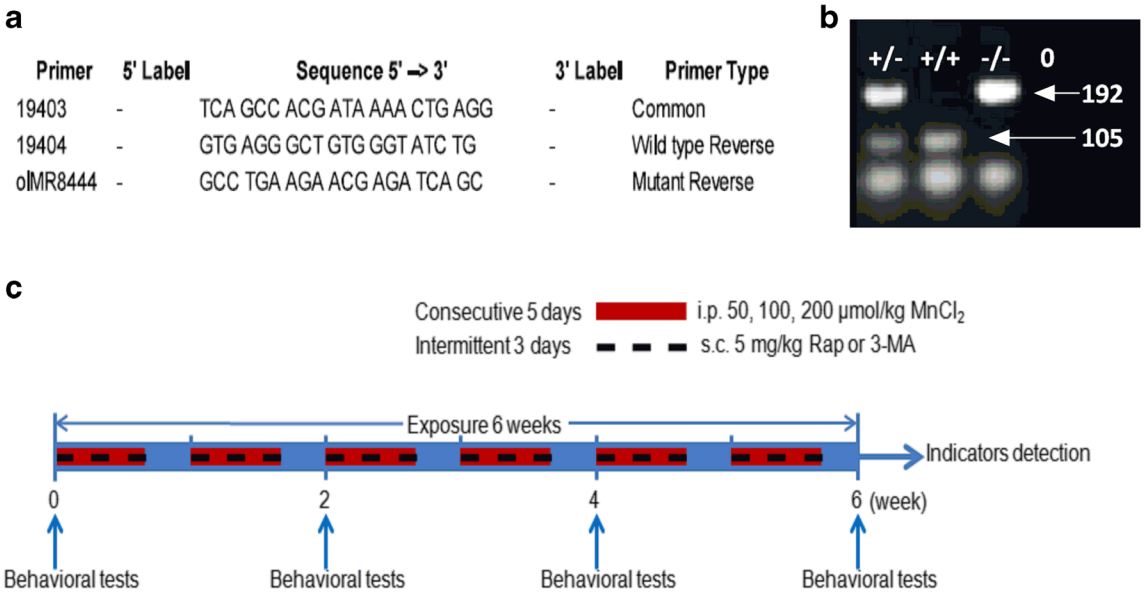

Fig. 1 The experimental procedure of this study. **a** The primers used for genotype identification in this study were shown. **b** Genotyping of wild-type (+/+: α-Syn$^{+/+}$ mice; 105 bp), α-Syn homozygous knock out (−/−: α-Syn$^{-/-}$ mice; 192 bp), heterozygous (+/−: common mice; 105~192 bp), and negative control (0) were shown. **c** Ten-week-old homozygous α-Syn$^{-/-}$ and α-Syn$^{+/+}$ mice from the same generation were exposed to $MnCl_2$ via i.p. for successive 5 days a week till the behavioral abnormalities were observed by behavioral tests (the whole exposure duration of $MnCl_2$ lasted 6 weeks totally). For drug pretreatment groups, α-Syn$^{+/+}$ mice were subjected to Rap (3-MA) via s.c. for interval 3 days a week in the same period of exposure to Mn. After accomplishment of behavioral tests, the brain was obtained to detect the relevant indicators

pretreated groups (Rap + Mn and 3-MA + Mn). To minimize the harm of mice, the manner of pretreatment (5 mg/kg Rap or 3-MA) were conducted by subcutaneous injection (s.c.) for three intermittent days, 2 h before i.p. injection with NaCl solution or 200 μmol/kg $MnCl_2$ (Matsushita et al. 2016; Pan et al. 2017). The whole exposure of animals was 6 weeks. The detailed experimental procedure was illustrated in Fig. 1c. The injection volume was 5 mL/kg body weight. The mice were bred at ambient temperature (22–23 °C) and humidity-controlled room.

Behavioral Tests

Open Field Test

Mice were placed in the center of a square box (50 cm × 50 cm × 50 cm) that divided into 16 quadrants. Firstly, these mice were adapted to the unacquainted environment for 2 min. Then, motor activities were recorded during a 5-min session by EthoVision XT 11.5 (Noldus, Netherlands) software. Total distance (cm) and rearing number (*n*) were used to assess the spontaneous locomotor activity of animals (Li et al. 2018).

Forced Swim Test

Forced swim test was carried out to observe the motor coordination ability of mice. Briefly, the mice were placed individually in water tank (100 cm × 50 cm × 30 cm) containing water (25 ± 1 °C), to be forced to swim from the one side to another side. During a 5-min session, immobility time (s) (floating without struggling or exhibiting no valid movements with their forepaws) was recorded manually (Li et al. 2018).

Static Weight-Bearing Assessment

The incapacitance meter was applied to measure static weight bearing of mice. The hind limbs of mice were set individually on load cells. The contralateral hind limbs weight difference (g) was manually recorded when the animals stabilized its positioning.

Grasping Strength

Mice were positioned on the wire grid (8 cm × 14 cm) connected to an ordinary electronic scale, and allowed to grasp the grip while being dragged the tail with increasing firmness till they loosened their grip. Each mouse was tested three times and the grasping strength (g) was noted by the scale at the precise moment of loosening. The mean grasping strength (g) was calculated automatically.

Measurement of Mn Contents in Striatum

A sample of striatum tissue from each group was wet-digested with 0.5 mL HNO_3 (70% HNO_3 for trace metal analysis). Then the samples were eluted with 0.5 mL 30% H_2O_2 solution

and the solution was utterly evaporated. The precipitate was dissolved in 5 mL deionized water and analyzed by a HITACHI 180-80 atomic absorption spectrometry system (Wang et al. 2017a). Concentrations were measured using a standard calibration curve.

Alpha-Synuclein Oligomerization Assay

The detection of α-Syn oligomers was according to our previous study (Xu et al. 2015). Briefly, after normalization of the protein concentration, the fresh protein samples (without ultrasound and boiling) from striatum tissue of each group were separated by a 4–20% non-denaturing polyacrylamide gradient gel (Thermo Fisher Scientific, USA) and then electrotransferred onto PVDF membranes (Immobilon-P^{SQ}, Millipore). The membranes were incubated with mouse α-Syn primary monoclonal antibody (1:500, Abcam Ltd., ab1903) overnight at 4 °C. Protein bands were visualized by chemiluminescent detection system (Pierce) and quantified by ImageJ.

Western Bolt Analysis

Protein extraction and immunoblot method were according to our previous study (Xu et al. 2014b). The following primary antibodies were used: Beclin1 (1:1000, rabbit polyclonal, Abcam Ltd., ab62557), LC3B (1:1000, rabbit polyclonal, Abcam Ltd., ab48394), p62 (1:1000, mouse monoclonal, Abcam Ltd., ab56416), Lamp 2A (1:1000, rabbit polyclonal, Abcam Ltd., ab18528), HSC70 (1:1000, mouse monoclonal, Abcam Ltd., ab2788), and β-actin (1:1000, rabbit polyclonal, Cell Signaling, ab4967). The expression of protein was detected by ECL chemiluminescent detection system and normalized to β-actin. The intensity of protein bands were quantified relatively by detecting the mean gray value by ImageJ (ImageJ, NIH, Bethesda, MA, USA).

Quantitative Real-Time PCR Analysis

Total RNA of striatum tissue was extracted using Trizol reagent (TaKaRa Biotech. Co. Ltd., China), and was reverse-transcribed using PrimeScript® RT Enzyme Mix I (TaKaRa Biotech. Co. Ltd., China). Quantitative real-time PCR was performed on ABI 7500 Real-Time PCR System (Applied Biosystems, USA) using *SYBR® Premix* Ex TaqTM II kit (TaKaRa Biotech. Co. Ltd., China). The final reaction mixture volume and reaction condition were the same as our previous study (Xu et al. 2014a). The primers used in this study are shown in Table 1 (Koga et al. 2011; Massey et al. 2006; Xu et al. 2015; Yasuhara et al. 2011). *β-actin* was used as an endogenous control. The results were calculated by the $2^{-\Delta\Delta Ct}$ method.

Table 1 Primer sequences used for the amplification of each gene in this study

Target	Primer	Sequence(5′-3′)
α-synuclein	Sense	CACAAGAGGGAATCCTGGAA
	Anti-sense	TCATGCTGGCCGTGAGG
Lamp 2A	Sense	GCAGTGCAGATGAAGACAAC
	Anti-sense	AGTATGATGGCGCTTGAGAC
HSC70	Sense	AGCTGCCTGGCATTTGTGTG
	Anti-sense	GTGCGGTTACCCTGGTCATTG
β-actin	Sense	GGAGATTACTGCCCTGGCTCCTA
	Anti-sense	GACTCATCGTACTCCTGCTT GCTG

Co-Immunoprecipitation of Lamp 2A with HSC70 and Alpha-Synuclein

A co-immunoprecipitation (Co-IP) assay was performed as described previously (Xu et al. 2015). After protein concentration normalization, the fresh protein samples from striatum tissue of each group were incubated with rabbit polyclone anti-Lamp 2A (1:40, Abcam Ltd., ab18528), mouse anti-HSC70 (1:50, Abcam Ltd., ab2788), or mouse anti-α-Syn (1:50, Abcam Ltd., ab1903) monoclonal antibody at 4 °C overnight to form antigen-antibody complex. Then immunomagnetic beads were pre-treated according manufacturer's instruction and re-suspended in binding buffer (containing 50 mM Tris, 150 mM NaCl, 0.2% Triton-100, pH 7.5). The antigen-antibody complex solution was added into binding buffer, incubated with beads for 2 h. The beads-antigen-antibody complex was collected by magnetic separation and loaded onto a 10% SDS-PAGE and electrotransferred onto PVDF membrane. Membrane blots were probed with mouse anti-HSC70 (1:1000, Abcam Ltd., ab2788), mouse anti-α-Syn (1:500, Abcam Ltd., ab1903), or rabbit anti-Lamp 2A (1:1000, Abcam Ltd., ab18528) antibodies and visualized using chemiluminescent detection system.

Immunofluorescence of Lamp 2A with HSC70 and Alpha-Synuclein

After fixed with paraformaldehyde, the serial coronary brain frozen slices (7 μm thickness) were directly mounted on slides and penetrated with 0.5% Triton. Normal sheep serum was used to blocked non-specific sites. Then, the slices were incubated with these primary antibodies overnight at 4 °C: Lamp 2A rabbit primary antibody (1:200, Abcam Ltd., ab18528) and HSC70 mouse primary antibody (1:200, Abcam Ltd., ab2788), Lamp 2A rabbit primary antibody (1:200, Abcam Ltd., ab18528), and α-Syn mouse primary antibody (1:50, Abcam Ltd., ab1903). After being rinsed with PBS, the slices were incubated with Alexa Fluor 488-labeled donkey anti-

rabbit secondary antibody and 594-labeled donkey anti-mouse secondary antibody (1:500, Molecular Probes, Invitrogen, Carlsbad, CA) in darkness for 2 h at room temperature. Olympus confocal microscope (FV 1000S-IX81, Olympus, Japan) was applied to examine the fluorescent signal. Colocalization was assessed by calculating the Pearson's correlation coefficient using ImageJ.

Apoptosis Assays

The apoptosis was detected by flow cytometry (FCM) according to previous description (Yuan et al. 2016). After 20 mg of the striatum tissue from four mice per group made into single cell suspension, the cells were dyed with Annexin V-FITC and propidium iodide (PI) according to the producer's manual and the fluorescent signals were detected by a flow cytometer (BD FACSCanto CantoII, USA). The early apoptosis percentage of cells (Annexin V^+ /PI^-, Q4) was automatically recorded.

MDC Staining of Autophagic Vacuoles

After striatum tissues made into cell suspension, the autofluorescent compound monodansylcadaverine (MDC) was used to stain autophagic vacuoles (Ding et al. 2016). The cell suspension were incubated with 0.05 mM MDC in PBS at 37 °C in the dark for 45 min, then washed three times with PBS. The incidence of autophagy (%) and mean fluorescence intensity (% of control) were analyzed by Flow cytometer (BD FACSCanto CantoII, USA).

Transmission Electron Microscopy

The formation of autophagosome in neuron was observed by transmission electron microscopy. After mice were anesthetized by 10% chloral hydrate, the striatum tissue was rapidly trimmed into 1-mm^3 tissue on ice and then fixed in 2.5% glutaraldehyde phosphoric acid for 2 h. The trimmed tissue sequentially undergone washed in PBS, post-fixed in 1% osmium tetroxide for 2 h, dehydrated with gradient alcohol, embedded, polymerized, trimmed and sectioned into slices, and stained with uranyl acetate and lead citrate. Finally, 12 pictures per group of the ultrastructural features in neurons were taken at × 15,000 magnification by transmission electron microscopy (H-600-4, Hitachi).

Statistical Analysis

All statistical analyses were carried out by SPSS 18.0 software. Experimental data were represented as mean ± standard error of mean (SE). Two-way ANOVA, followed by the Student-Newman-Keuls test (q test) for multiple comparisons, was conducted to assess the effect of Mn factor and genotype factor on the results. Differences between α-$Syn^{+/+}$ and α-$Syn^{-/-}$ mice were analyzed by two-tailed, unpaired Student's t test. As for Rap/3-MA pretreatment, statistical analysis was performed by one-way ANOVA followed by Student-Newman-Keuls test. A P value < 0.05 indicated statistical significance.

Results

Behavioral Abnormalities Induced by Mn in Both α-$Syn^{+/+}$ and α-$Syn^{-/-}$ Mice

We observed obvious motor and behavioral deficits till Mn exposure for 6 weeks in both α-$Syn^{+/+}$ and α-$Syn^{-/-}$ mice, which were shown in Fig. 2 (Supplemental Table S1–2). Open field test showed that total distance and rearing number in 50–200 μmol/kg Mn-treated α-$Syn^{+/+}$ and α-$Syn^{-/-}$ mice were significantly decreased compared to their controls, respectively (Mn factor $F_{(\text{total distance})} = 405.35$, $P < 0.05$, genotype factor $F_{(\text{total distance})} = 38.77$, $P < 0.05$, genotype vs. Mn interaction $F_{(\text{total distance})} = 4.05$, $P < 0.05$; Mn factor $F_{(\text{rearing number})} = 78.32$, $P < 0.05$, genotype factor $F_{(\text{rearing number})} = 4.19$, $P < 0.01$, genotype vs. Mn interaction $F_{(\text{rearing number})} = 1.19$, $P > 0.05$; Fig. 2a, b). Compared to Mn-treated α-$Syn^{+/+}$ mice, there was a significant decrease of total distance in Mn-treated α-$Syn^{-/-}$ mice ($P < 0.01$; Fig. 2a). Rearing number in 200 μmol/kg Mn-treated α-$Syn^{+/+}$ mice was more decreased than that in 200 μmol/kg Mn-treated α-$Syn^{-/-}$ mice ($P < 0.05$; Fig. 2b). Immobility time in forced swimming test showed an upward trend in Mn-treated α-$Syn^{+/+}$ and α-$Syn^{-/-}$ mice (Mn factor $F = 436.75$, $P < 0.01$, genotype factor $F = 54.45$, $P < 0.01$, genotype vs. Mn interaction $F = 6.43$, $P < 0.01$; Fig. 2c); further, there was a significant difference between Mn-treated α-$Syn^{+/+}$ and α-$Syn^{-/-}$ mice ($P < 0.01$; Fig. 2c). With increasing Mn dose, grasping strength of α-$Syn^{+/+}$ and α-$Syn^{-/-}$ mice were significantly strengthened (Mn factor $F = 18.10$, $P < 0.01$, genotype factor $F = 10.26$, $P < 0.01$, genotype vs. Mn interaction $F = 1.28$, $P > 0.05$), and α-$Syn^{-/-}$ mice exhibited more abnormal limb-clasping response with stiffness when they were suspended by their tails than α-$Syn^{-/-}$ mice in 100 and 200 μmol/kg Mn treatment ($P < 0.05$; Fig. 2d). In static weight-bearing test, the contralateral hind paw weight difference increased significantly in Mn-treated α-$Syn^{+/+}$ (100, 200 μmol/kg) and α-$Syn^{-/-}$ (50–200 μmol/kg) mice compared to controls (Mn factor $F = 106.09$, $P < 0.01$, genotype factor $F = 11.62$, $P < 0.01$, genotype vs. Mn interaction $F = 5.83$, $P < 0.01$; Fig. 2e). There was a significant difference in this indicator between α-$Syn^{+/+}$ and α-$Syn^{-/-}$ mice in 200 μmol/kg Mn treatment ($P < 0.05$; Fig. 2e). These data suggested that Mn could impair motor coordination, balance, and grasping strength in both α-$Syn^{+/+}$ and α-$Syn^{-/-}$ mice, and induce greater behavioral effects in α-$Syn^{-/-}$ mice compared with α-$Syn^{+/+}$ mice. These behavioral

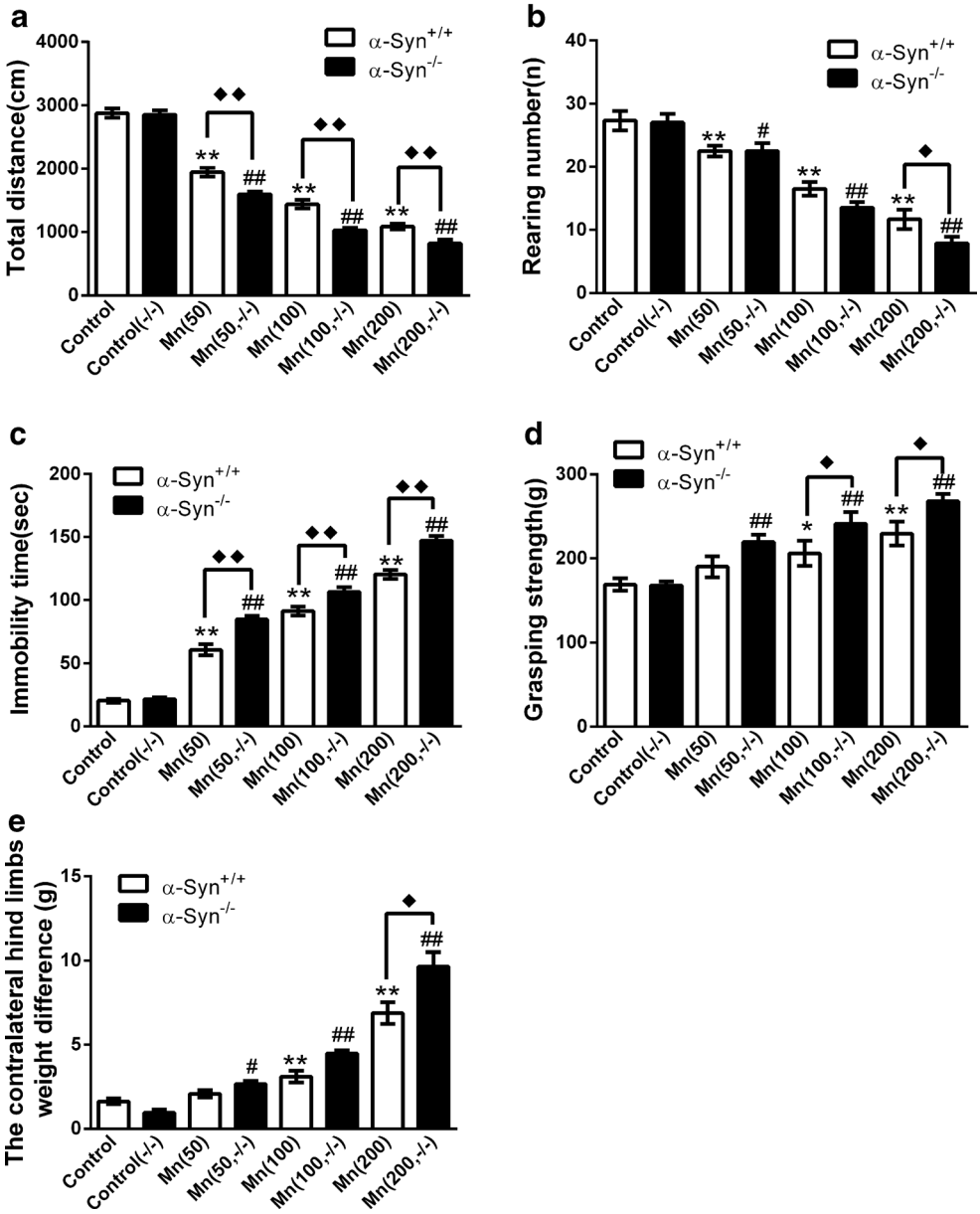

Fig. 2 Summary of the performance of α-Syn$^{+/+}$ and α-Syn$^{-/-}$ mice on behavioral tests evaluating the motor capacity 6 weeks after Mn exposure. **a**, **b** Total distance and rearing number were decreased by Mn treatment in the open field test. **c** Immobility time was increased by Mn treatment in forced swim test. **d** Grasping strength was enhanced in Mn-treated α-Syn$^{+/+}$ and α-Syn$^{-/-}$ mice. **e** Mn-treated α-Syn$^{+/+}$ and α-Syn$^{-/-}$ mice performed the poor ability of balance in static weight-bearing test. *$P < 0.05$ and **$P < 0.01$ vs. control; #$P < 0.05$ and ##$P < 0.01$ vs. control (−/−); ◆$P < 0.05$ and ◆◆$P < 0.01$ α-Syn$^{-/-}$ vs. α-Syn$^{+/+}$ mice. $n = 6$ per group

abnormalities indicated our mice models of manganism were successfully established.

Alpha-Synuclein Ameliorated Mn-Induced Autophagy and Apoptosis

Previous study reported that Mn could pass through blood-brain barrier (BBB) storing central nervous system (CNS), particularly globus pallidus, striatum, and substantia nigra (Horning et al. 2015). In this study, we detected the level of Mn in striatum to reflect the absorption situation of the metal in Mn-treated groups. Statistical comparisons revealed that Mn concentration in striatum of Mn-treated α-Syn$^{+/+}$ and α-Syn$^{-/-}$ mice (50–200 μmol/kg) gradually increased in a dose-dependent manners ($r = 0.895$, $P < 0.01$, $r_{(-/-)} = 0.926$, $P < 0.01$; Fig. 3a). Mn concentration in striatum in Rap and 3-MA pretreatment were also significantly higher than those in control group (5.1- and 5.2-fold of the control; respectively, $P < 0.01$; Fig. 7a), which indicated that the pretreatment with Rap or 3-MA had no effects on the brain accumulation of Mn. The result of apoptotic in this study demonstrated that Mn damaged nerve cell, which was consistent with previous report (Pfalzer and Bowman 2017) (Mn factor $F = 96.02$, $P < 0.01$, genotype factor $F = 18.31$, $P < 0.01$, genotype vs. Mn interaction $F = 3.33$, $P < 0.05$; Fig. 3b; Supplemental Fig. S1). Another important finding was the significant difference in apoptotic between α-Syn$^{-/-}$ mice and α-Syn$^{+/+}$ mice in 100 and 200 μmol/kg Mn treatment ($P < 0.05$; Fig. 3b), suggesting that α-Syn$^{-/-}$ mice more susceptible to Mn than α-Syn$^{+/+}$ mice.

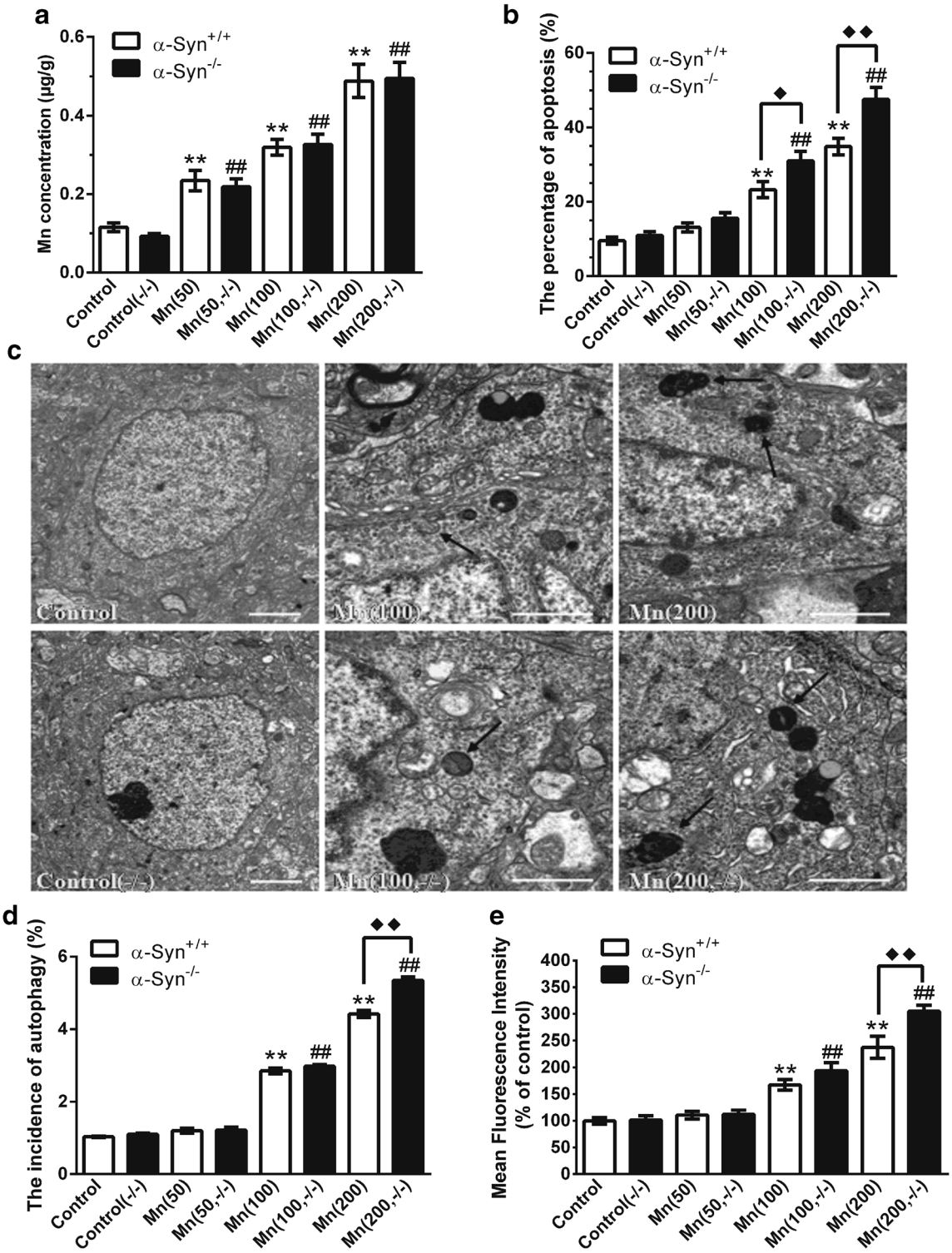

Fig. 3 Alpha-synuclein ameliorated Mn-induced autophagy and apoptosis. **a** The increase accumulation of Mn concentration in striatum in Mn-treated α-Syn$^{-/-}$ and α-Syn$^{+/+}$ mice were measured. **b** Apoptosis of both Mn-treated α-Syn$^{-/-}$ and α-Syn$^{+/+}$ mice were analyzed using flow cytometry. **c** TEM images show autophagy vesicle in neurons of both Mn-treated α-Syn$^{-/-}$ and α-Syn$^{+/+}$ mice and controls. Arrows indicate autophagosomes and autolysosomes. The scale bar: 2 μm (controls) and 1 μm (Mn-treated groups). **d**, **e** The incidence of autophagy and mean fluorescence intensity of α-Syn$^{-/-}$ and α-Syn$^{+/+}$ mice was detected by MDC-labeled autophagy vesicles using flow cytometry. Statistics are depicted as mean ± SE, $^{**}P < 0.01$ vs. control; $^{\#\#}P < 0.01$ vs. control (−/−); $^{\blacklozenge}P < 0.05$ and $^{\blacklozenge\blacklozenge}P < 0.01$ α-Syn$^{-/-}$ vs. α-Syn$^{+/+}$ mice; $n = 4$ per group

Considering a close association between autophagy and apoptosis, we carried out a series of detections to assess autophagy. Firstly, few autophagosomes and phagophores observed by electron microscopy were presented in control groups (Fig. 3c). In contrast, an obvious increase of autophagosomes and autolysosomes that contained dense granules were observed in 100 and 200 μmol/kg Mn-treated α-Syn$^{-/-}$ and α-Syn$^{+/+}$ mice (Fig. 3c). To better assess the level of autophagy, we further used FCM to detect the incidence of autophagy and the mean fluorescence intensity by MDC-labeled autophagosome. Statistical analysis revealed that 100 and 200 μmol/kg Mn treatment could activate autophagy in both α-Syn$^{-/-}$ and α-Syn$^{+/+}$ mice(Mn factor $F_{(\text{incidence of autophagy})} = 1382.30$, $P < 0.01$, genotype factor $F_{(\text{incidence of autophagy})} = 35.80$, $P < 0.01$, genotype vs. Mn interaction $F_{(\text{incidence of autophagy})} = 20.32$, $P < 0.01$; Mn factor $F_{(\text{mean fluorescence intensity})} = 93.03$, $P < 0.01$, genotype factor $F_{(\text{mean fluorescence intensity})} = 8.89$, $P < 0.01$, genotype vs. Mn interaction $F_{(\text{mean fluorescence intensity})} = 3.62$, $P < 0.05$; Fig. 3d, e), and this effect (activated autophagy) on α-Syn$^{-/-}$ mice was more drastic than α-Syn$^{+/+}$ mice in 200 μmol/kg Mn treatment ($P < 0.01$; Fig. 3d, e), indicating an excessive autophagy in α-Syn$^{-/-}$ mice induced by 200 μmol/kg Mn treatment. These above results suggested that α-Syn might be involved in the regulation of Mn-induced excessive autophagy and apoptosis.

Activation of CMA Pathway by Mn Was Independent of α-Syn

CMA is regarded to be a selective mechanism for the degradation of misfolded/unfolded protein by which chaperone protein HSC70 directly recognizes CMA substrate protein and transports them to the lysosomes for Lamp 2A-mediated degradation. To explore the activation state of CMA, we detected the levels of Lamp 2A and HSC70 mRNA and protein expression in Mn-treated α-Syn$^{+/+}$ and α-Syn$^{-/-}$ mice. The results of Fig. 4a–c revealed that the levels of Lamp 2A and HSC70 mRNA and protein expression both significantly increased in response to Mn treatment (50–200 μmol/kg) without difference between α-Syn$^{+/+}$ and α-Syn$^{-/-}$ mice (Mn factor $F_{(\text{Lamp2a mRNA})} = 14.57$, $P < 0.01$, genotype factor $F_{(\text{Lamp2a mRNA})} = 0.328$, $P > 0.05$, genotype vs. Mn interaction $F_{(\text{Lamp2a mRNA})} = 0.27$, $P > 0.05$; Mn factor $F_{(\text{HSC70 mRNA})} = 10.53$, $P < 0.01$, genotype factor $F_{(\text{HSC70 mRNA})} = 0.009$, $P > 0.05$, genotype vs. Mn interaction $F_{(\text{HSC70 mRNA})} = 0.339$, $P > 0.05$; Mn factor $F_{(\text{Lamp2a protein})} = 40.23$, $P < 0.01$, genotype factor $F_{(\text{Lamp2a protein})} = 0.61$, $P > 0.05$, genotype vs. Mn interaction $F_{(\text{Lamp2a protein})} = 0.92$, $P > 0.05$; Mn factor $F_{(\text{HSC70 protein})} = 14.71$, $P < 0.01$, genotype factor $F_{(\text{HSC70 protein})} = 1.197$, $P > 0.05$, genotype vs. Mn interaction $F_{(\text{HSC70 protein})} = 0.222$, $P > 0.05$). Furthermore, we investigated the interaction of HSC70 and Lamp 2A by using laser scanning confocal microscopy and Co-IP. As shown in Fig. 4d, the brain slices from α-Syn$^{+/+}$ and α-Syn$^{-/-}$ mice were double stained by anti-HSC70 antibody conjugated with Alexa Fluor 594 and anti-Lamp 2A antibody conjugated with Alexa Fluor 488. The overlay images showed that HSC70 colocalized well with Lamp 2A in 50 μmol/kg Mn-treated α-Syn$^{+/+}$ and α-Syn$^{-/-}$ mice, compared to their controls (Fig. 4d, e). Similarly, the analysis by Co-IP revealed that the interaction of Lamp 2A and HSC70 significantly enhanced in Mn treated α-Syn$^{+/+}$ and α-Syn$^{-/-}$ mice (Fig. 4f, g). These data indicated that activation of CMA pathway by Mn was independent of α-Syn. Next, we further examined the effect of CMA on Mn-induced α-Syn overexpression. As expected, Mn significantly increased the levels of both α-Syn mRNA and protein expression in α-Syn$^{+/+}$ mice (Fig. 5a–c). Besides, the enhanced colocalization of Lamp 2A (labeled—Alexa Fluor 488) with α-Syn (labeled—Alexa Fluor 594) was induced by 50 μmol/kg Mn treatment (Fig. 5d, e). Consistently, the analysis of Co-IP further confirmed the increased interaction of Lamp 2A and α-Syn in Mn treatment ($P < 0.01$, Fig. 5f, g), indicating that CMA pathway might be involved in the degradation of α-Syn.

α-Syn Ameliorated Excessive Autophagy Induced by High Dose Mn

Macroautophagy can complement the proteasome and CMA, which is deemed to be a non-selective mechanism for the turnover of proteins (Jackson and Hewitt 2016). Autophagy functions as a physiologic stress response and quality control mechanism within mammalian cells (Ravanan et al. 2017). To investigate the effect of Mn on macroautophagy, we detected macroautophagy associated with protein expression (Beclin1, LC3-II/I, and p62) in both α-Syn$^{+/+}$ and α-Syn$^{-/-}$ mice. Beclin1, a protein with a key role in autophagy, is involved in the recruitment of membranes to form autophagosomes (Wirawan et al. 2012). LC3-II/I, generally as an autophagy marker, constantly exists on phagophore and autophagosomal membranes. p62 is an ubiquitin-binding protein that acts as a receptor for autophagic substrates (Janda et al. 2015). The Western blot analysis showed that a significant increase of Beclin1 in Mn-treated (100, 200 μmol/kg) α-Syn$^{+/+}$ and α-Syn$^{-/-}$ mice (Mn factor $F = 77.29$, $P < 0.01$, genotype factor $F = 0.88$, $P > 0.05$, genotype vs. Mn interaction $F = 0.08$, $P > 0.05$), an increase of LC3-II/I in Mn-treated (200 μmol/kg) α-Syn$^{+/+}$ and (100, 200 μmol/kg) α-Syn$^{-/-}$ mice (Mn factor $F = 41.53$, $P < 0.01$, genotype factor $F = 32.02$, $P < 0.01$, genotype vs. Mn interaction $F = 9.82$, $P < 0.01$), and a reduction of p62 in both Mn-treated (50–200 μmol/kg) α-Syn$^{+/+}$ and α-Syn$^{-/-}$ mice, compared to controls (Mn factor $F = 37.41$, $P < 0.01$, genotype factor $F = 0.48$, $P > 0.05$, genotype vs. Mn interaction $F = 1.27$, $P > 0.05$; Fig. 6a, b). The above results suggested that Mn could activate

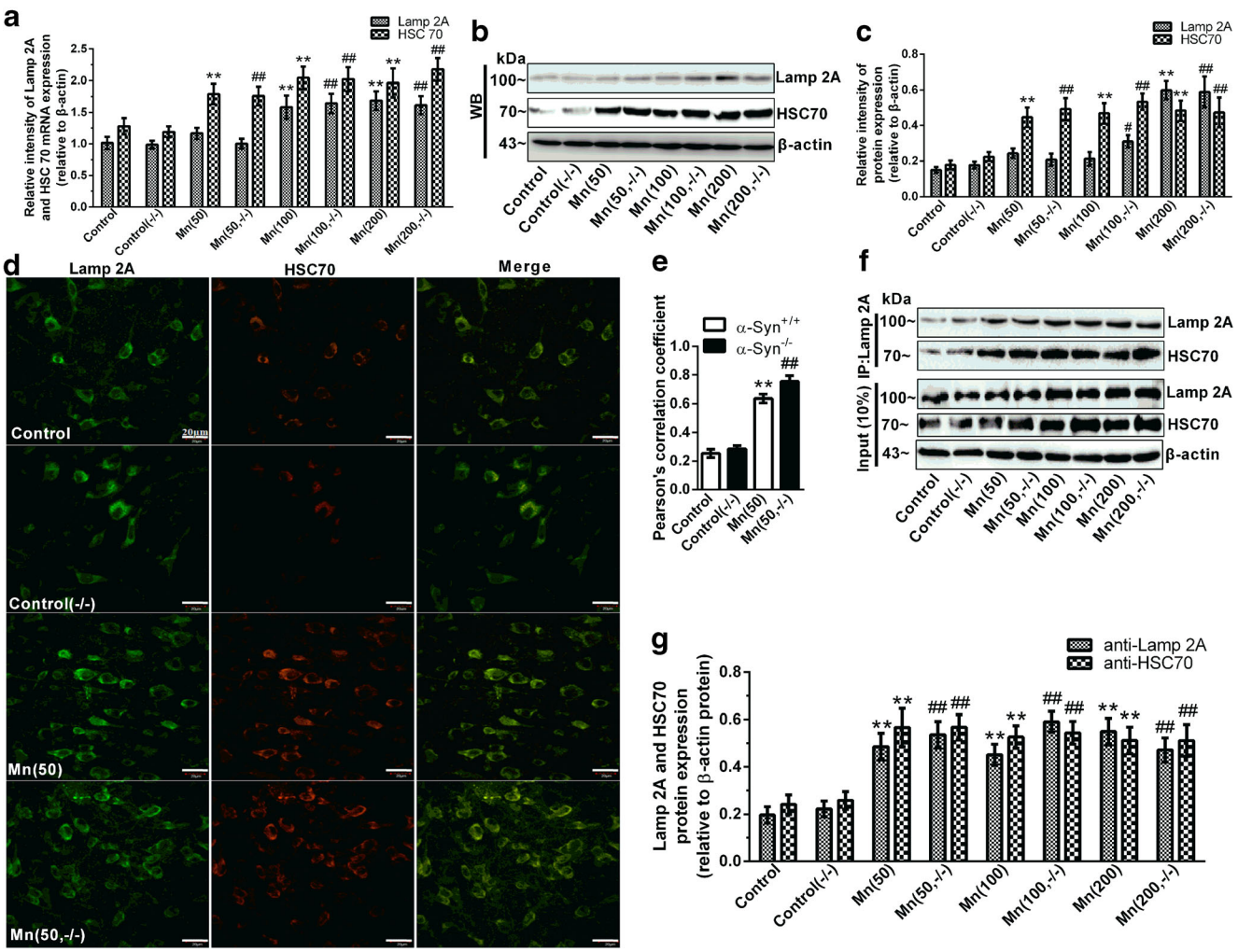

Fig. 4 Low dose Mn activated CMA pathway. **a**–**c** The levels of Lamp 2A and HSC70 mRNA and protein expression of α-Syn$^{+/+}$ and α-Syn$^{-/-}$ mice were shown. **d**, **e** The colocalization of Lamp 2A (green) and HSC70 (red) of 50 μmol/kg Mn treated α-Syn$^{+/+}$ and α-Syn$^{-/-}$ mice and their controls were examined by Olympus confocal microscope with the × 40 objective lens and assessed by calculating the Pearson's correlation coefficient. The scale bar: 20 μm. **f**, **g** The immunoprecipitation products and semi-quantitative analysis of Lamp 2A and HSC70 in α-Syn$^{+/+}$ and α-Syn$^{-/-}$ mice were shown. Lamp 2A was immunoprecipitated. Immunoprecipitates were analyzed by immunoblotting for Lamp 2A and HSC70. Statistics are depicted as mean ± SE, $^{**}P < 0.01$ vs. control; $\#P < 0.05$ and $\#\#P < 0.01$ vs. control (−/−); $n = 4$ per group

macroautophagy in both α-Syn$^{+/+}$ and α-Syn$^{-/-}$ mice. Of note, there was a significant difference in LC3-II/I expression between α-Syn$^{+/+}$ and α-Syn$^{-/-}$ mice in 100 and 200 μmol/kg Mn treatments ($P < 0.01$; Fig. 6a, b). The above results suggested that the important role of α-Syn in ameliorating Mn-induced excessive autophagy.

Macroautophagy Regulated Mn-Induced Alpha-Synuclein Oligomerization and Its Neurotoxicity

To explore the effect of autophagy on Mn-induced α-Syn oligomerization and neurotoxicity, we applied Rap and 3-MA to pretreat α-Syn$^{+/+}$ mice. Statistical analysis of MDC-labeled autophagy vesicles showed that the Rap pretreatment could significantly activate autophagy, and yet inhibition induced by 3-MA pretreatment (Fig. 7b, c). Consistent with this, the Western blotting analysis showed that the Rap pretreatment could effectively increase the protein expression of Beclin1 and LC3-II/I with p62 reduction, whereas 3-MA pretreatment induced opposite effects, compared to 200 μmol/kg Mn treatment (Fig. 7d, e), which suggested that Rap properly upregulated autophagy and yet 3-MA downregulated autophagy in this study. Next, we found that Rap or 3-MA pretreatment had no effect on the increase of *α-Syn* mRNA level induced by Mn (Fig. 7f). A significant decrease of α-Syn oligomers caused by Rap pretreatment and yet an obvious increase induced by 3-MA pretreatment compared to 200 μmol/kg Mn treatment (Fig. 7g, h). These results confirmed that upregulated autophagy by Rap could effectively

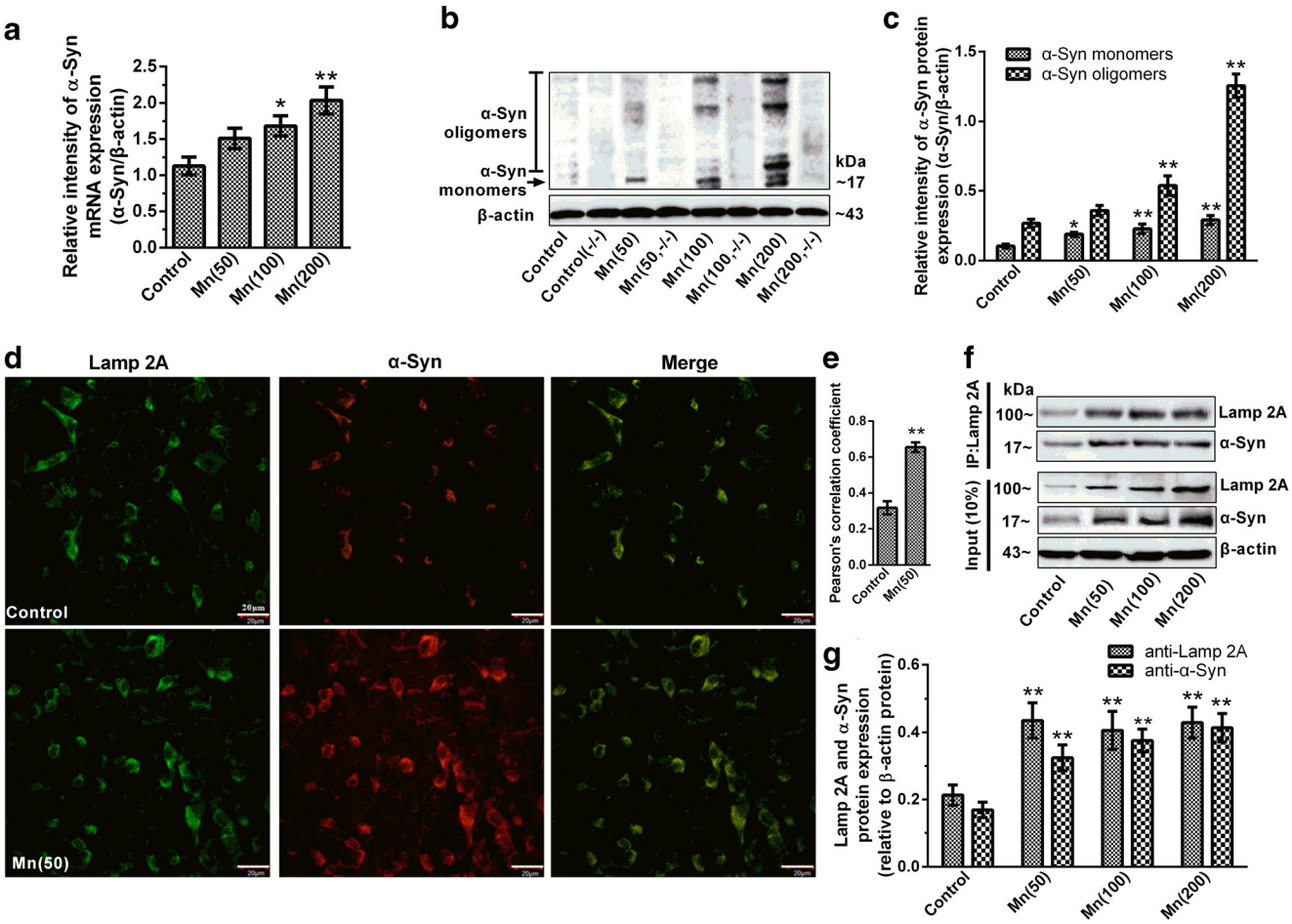

Fig. 5 CMA pathway involved in the degradation of α-Syn. **a**–**c** The levels of the α-Syn mRNA and protein expression of Mn-treated α-Syn$^{+/+}$ and α-Syn$^{-/-}$ mice were shown. **d**, **e** The colocalization of Lamp 2A (green) and α-Syn (red) of 50 μmol/kg Mn treated α-Syn$^{+/+}$ and the control were examined by Olympus confocal microscope with the × 40 objective lens and assessed by calculating the Pearson's correlation coefficient. The scale bar: 20 μm. **f**, **g** The immunoprecipitation products and semi-quantitative analysis of Lamp 2A and α-Syn in α-Syn$^{+/+}$ mice were shown. Lamp 2A was immunoprecipitated. Immunoprecipitates were analyzed by immunoblotting for Lamp 2A and α-Syn. $^{*}P < 0.05$ and $^{**}P < 0.01$ vs. control; $n = 4$ per group

promote the degradation of α-Syn oligomers, whereas 3-MA pretreatment caused the oligomers more accumulation upon Mn exposure. In conjunction, the result of apoptosis confirmed that Rap pretreatment partly attenuated Mn-induced apoptosis and yet 3-MA pretreatment aggravated Mn-induced apoptosis, compared to 200 μmol/kg Mn treatment (Fig. 7i; Supplemental Fig. S2). These data indicated the important role of autophagy in ameliorating Mn-induced α-Syn oligomerization and neurotoxicity.

Discussion

Our results demonstrated that the physiological role of α-Syn could ameliorate Mn-induced excessive autophagy and neurocytes injury, as evidenced by α-Syn$^{+/+}$ vs. α-Syn$^{-/-}$ mice. Furthermore, another important finding of the current study was the important role of upregulation autophagy in ameliorating Mn-induced α-Syn oligomerization and neurocytes injury proved by the application of Rap and 3-MA in α-Syn$^{+/+}$ mice. Taken together, these results further indicated that α-Syn oligomerization exerted more detrimental neurotoxicity role than excessive autophagy in the process of Mn-induced neurocytes injury (Fig. 8).

It is well known that overexposure to Mn could result in a neurodegenerative disorder known as 'manganism,' characterized by behavioral changes, tremors, difficulty walking, and slow and clumsy movements (Braak and Del Tredici 2017). In this study, open field test was used to assess spontaneous locomotor activities of the animals; forced swim test was employed to evaluate the ability of motor coordination; grasping strength was conducted to observe the flexibility of limbs; and measure of the contralateral hind limbs weight difference in static weight bearing test was used to evaluate the ability of balancing the load between both hind limbs (Rial et al. 2014; Tetreault et al. 2011; Wang et al. 2017b). Our

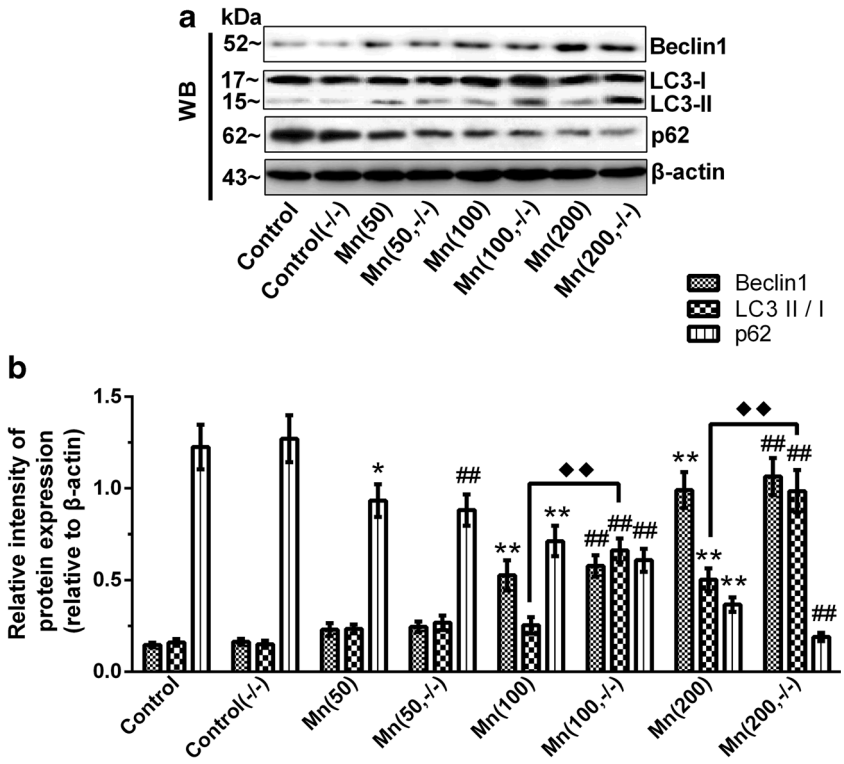

Fig. 6 α-Syn ameliorated excessive autophagy by high dose Mn. **a**, **b** The protein expressions of Beclin1, LC3-II/I and p62 in α-Syn$^{+/+}$ and α-Syn$^{-/-}$ mice determined by Western blotting and semi-quantitative analysis were shown. Statistics are depicted as mean ± SE from three independent tests, $*P < 0.05$ and $**P < 0.01$ vs. control; $\#\#P < 0.01$ vs. control (−/−); $\blacklozenge\blacklozenge P < 0.01$ α-Syn$^{-/-}$ vs. α-Syn$^{+/+}$ mice. $n = 4$ per group

results showed that abnormal behavioral changes were observed in both α-Syn$^{+/+}$ and α-Syn$^{-/-}$ mice till exposure to Mn (50–200 μmol/kg) for 6 weeks (i.e., the decreased total distance and rearing number, tested in an open-field; the increased immobility time, tested in forced swim test; the increased grasping strength, tested with the grasping strength test; and the increased contralateral hind limbs weight difference, tested in static weight bearing test). These above observations in mice reflected their poor capacity of locomotor activity, motor coordination, balance, and tetanic grasping performance, which suggested a behavioral dysfunction. The detrimental effect of Mn on behavioral changes might result from deficits in dopaminergic (DAergic) neurotransmission and eventual degeneration of these neurons (O'Neal and Zheng 2015). These behavioral changes indicated that our mice model of manganism was successfully established and provided ideal condition for further investigation. It is noteworthy that in the context of no difference in Mn concentration in striatum, we observed that there were significant differences in behavioral parameters (total distance, rearing number, immobility time, grasping strength, and the contralateral hind paw weight) and apoptosis between Mn-treated α-Syn$^{-/-}$ mice and α-Syn$^{+/+}$ mice, which indicated mice lack of α-Syn might be more susceptible to toxicants. This effect corroborates the notion of α-Syn as a Mn store, appearing to be neuroprotective against Mn-induced neurotoxicity (Peres et al. 2016). Besides this, many literatures have reported that Mn can cause the dopaminergic cell death through mitochondrial apoptosis pathway causing the release of cytochrome C, and activation of caspase-3/caspase-9 apoptosis signaling. Harischandra et al. (2015) found that α-Syn appeared to be protective against mitochondrial apoptosis early on, inhibited caspase-3/caspas-9 activation upon Mn exposure. They also reported many aspects about the neuroprotection of α-Syn at the early stages of Mn exposure, including attenuating the downstream apoptotic cascade, interfering with PKCδ by reducing its proteolytic cleavage and kinase activity, reducing p300 histone acetyltrasferase activity, retaining primary neuronal morphology.

Autophagy homeostasis is essential for maintaining cell homeostasis and ensures cell survival under stressful conditions. When imbalanced autophagy—either overactive or suppressed—occurs, the detrimental effect on neuron occurs, leading to cell damage or death (Xilouri et al. 2016). Recent evidence indicates that Mn could activate autophagic cell death in dopaminergic neurons (Zhang et al. 2013). Moreover, autophagy performed a protective role at early stage upon Mn exposure, while autophagy dysregulation at later phases induced dopaminergic neurodegeneration (Zhang et al. 2013). The results of Fig. 3d, e showed that the level of autophagy in α-Syn$^{-/-}$ mice was higher than α-Syn$^{+/+}$ mice in 200 μmol/kg Mn treatment, which hinted that α-Syn might ameliorate excess autophagy. In order to explore the effect of α-Syn on autophagy, we used α-Syn$^{-/-}$ and α-Syn$^{+/+}$ mice in the current study, which generated by homologous recombination and selected from the same generation (F6 generation owning stable genotypes) to avoid unknown variation in background strain, to demonstrate the important

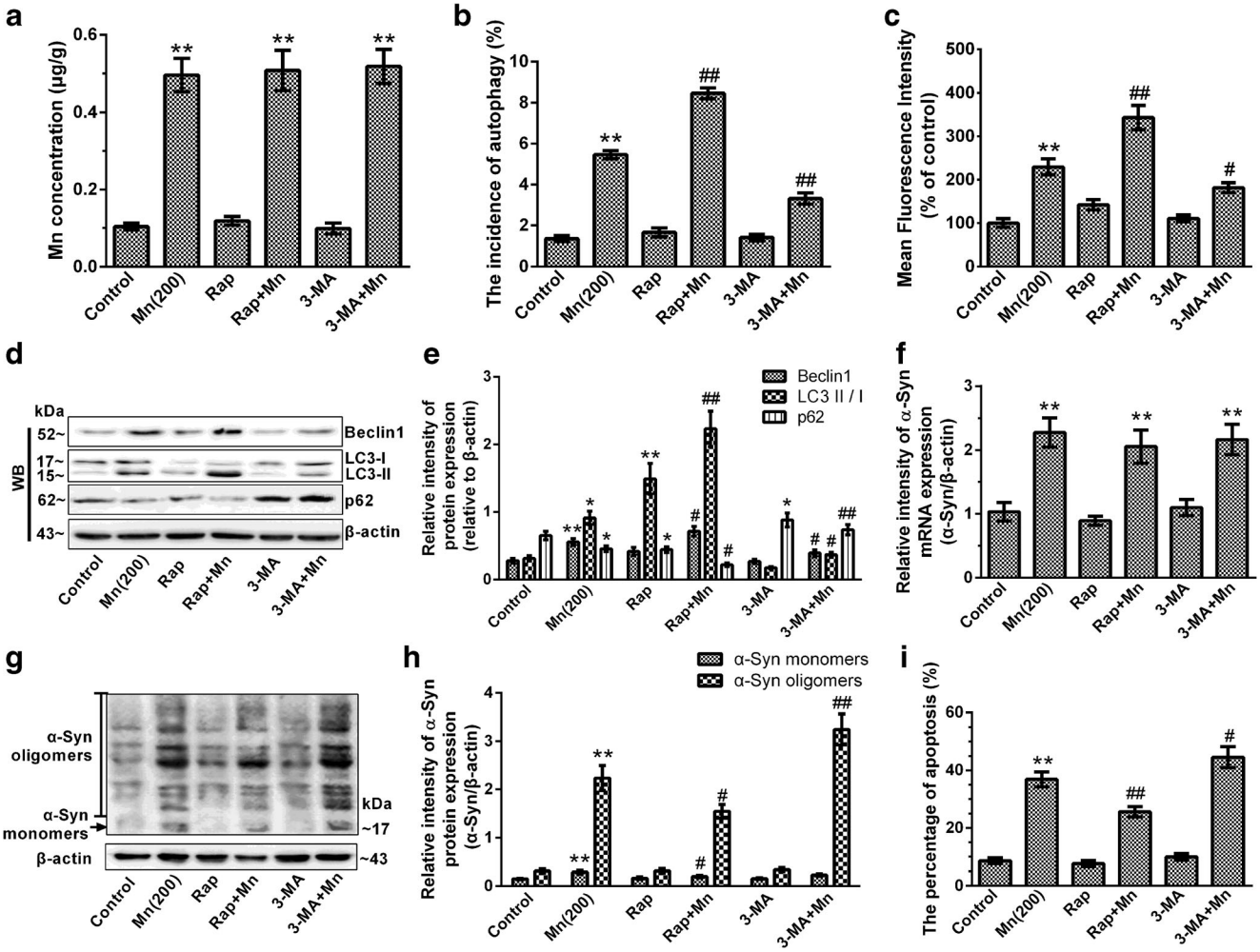

Fig. 7 Macroautophagy regulated Mn-induced alpha-synuclein oligomerization and its neurocytes injury. **a** Effects of Rap or 3-MA pretreatment on accumulation of Mn concentration in striatum were measured. **b**, **c** Effects of Rap or 3-MA pretreatment on Mn-induced autophagy occurrence were determined by flow cytometry. **d**, **e** The protein expressions and semi-quantitative analysis of Beclin1, LC3-II/I and p62 in 200 μmol/kg Rap and 3-MA pretreated α-Syn$^{+/+}$ mice were shown. **f**–**h** Effects of Rap or 3-MA pretreatment on the levels of α-Syn mRNA and protein expression was shown. **i** Effects of Rap or 3-MA pretreatment on Mn-induced nerve cells apoptosis. Statistics are depicted as mean ± SE from three independent tests. *$P < 0.05$ and **$P < 0.01$ vs. control; #$P < 0.05$ and ##$P < 0.01$ vs. Mn (200). $n = 4$ per group

role of α-Syn in ameliorating Mn-induced excessive autophagy and neurotoxicity by vs. α-Syn$^{+/+}$ mice. CMA and macroautophagy, as two important subtypes of autophagy, play a critical role in cellular quality control to protect neurons from many kinds of damage and disease, such as acute injury, chronic neurodegeneration, and brain tumors (Wu et al. 2015; Zhang et al. 2016). The activity of CMA can be modulated by the levels of Lamp 2A and HSC70 (Wu et al. 2015). In the present study, our findings demonstrated that exposure to Mn could induce activation of CMA pathway, which was supported by the increase in the levels of both Lamp 2A and HSC70 levels, and the enhanced colocalization and combination of both Lamp 2A and HSC70. In addition, CMA bases on the recognition of a specific amino acid sequence (KFERQ) to selectively degrade protein substrates (Wu et al. 2015). α-Syn, as one of the most containing the KFERQ-like motif FVKKDQ proteins, degrades partly depending on CMA pathway (Jackson and Hewitt 2016). Our results corroborated with previous findings (Wu et al. 2015), which demonstrated that CMA pathway might be involved in the degradation of Mn-induced α-Syn overexpression. Macroautophagy, a non-selective mechanism for the turnover of proteins, generally regarded to be crucial for the degradation of α-Syn oligomers and aggregates, since CMA is unable to deal with large protein species (Wu et al. 2015). Autophagy-associated proteins (ATG) encoded by autophagy-associated (*atg*) genes are tightly involved in the whole autophasosome formation process (Zhang et al. 2016). In the present study, we found that Mn could activate macroautophagy by increasing Beclin1, LC3-II/I, and decreasing autophagy substrates p62. Importantly, a more increase of LC3-II/I protein expression in Mn-treated α-Syn$^{-/-}$ mice than α-Syn$^{+/+}$ mice, indicating that

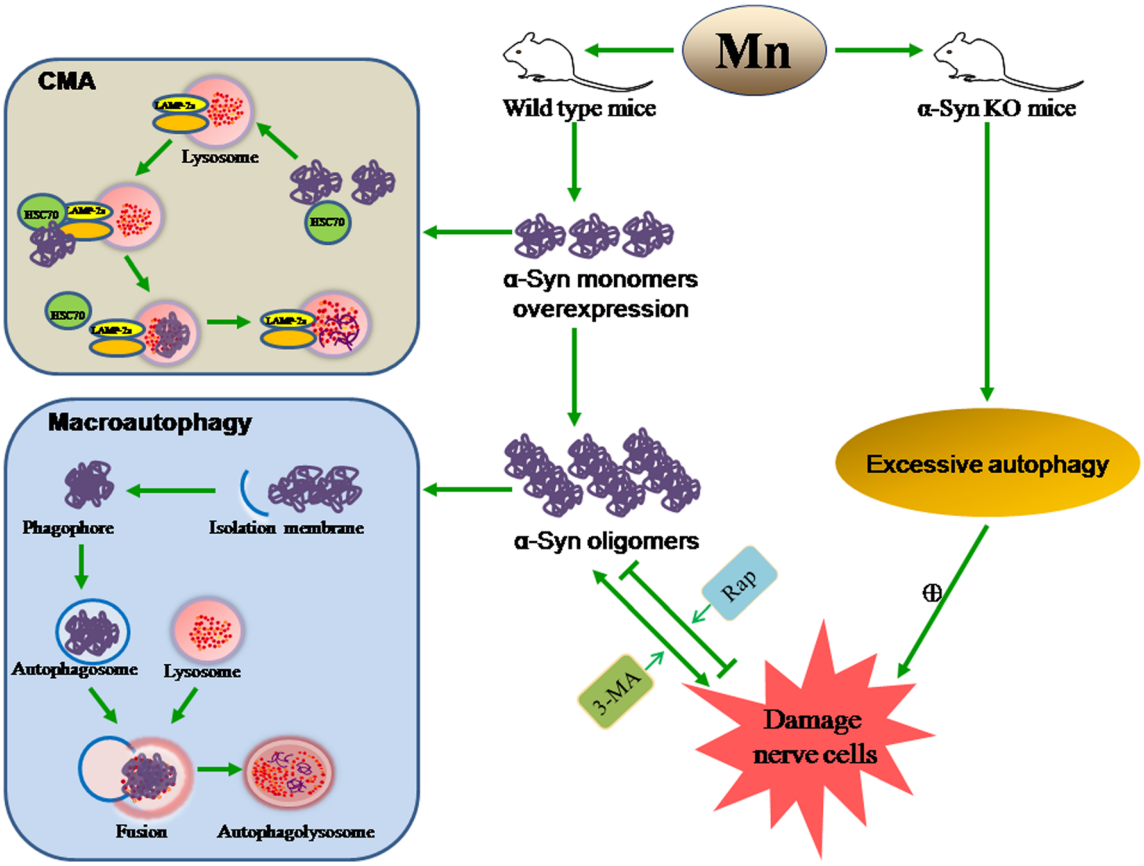

Fig. 8 Effect of the cross-talk between SNCA/α-synuclein oligomerization and autophagy on Mn-induced neurocytes injury. Mice lack of α-Syn performed excessive autophagy and apoptosis aggravation upon Mn exposure by vs. α-Syn$^{+/+}$ mice, which suggested the neuroprotective role of α-Syn in ameliorating Mn-induced excessive autophagy and neurocytes injury. On the other hand, autophagy (both macroautophagy and CMA) was involved in the degradation of Mn-induced α-Syn overexpression (monomers and oligomers). Upregulation (downregulation) of autophagy by Rap (3-MA) could ameliorate (exacerbate) Mn-induced α-Syn oligomerization and apoptosis, indicating the causative role of α-Syn in the development of Mn-induced neurodegenerative diseases

macroautophagy in α-Syn$^{-/-}$ mice was excessive activation by Mn, which was consistent with the above result of FCM detecting MDC-labeled autophagy vesicles.

In our previous study, we reported that Mn could promote α-Syn oligomerization in a dose-dependent manner through activation of iNOS and S-nitrosylation of protein disulfide isomerase inducing nitrosative stress in ER (Xu et al. 2014a). α-Syn oligomers perform neurotoxic effect to the cell via interaction with membranes (Gonzalez-Horta 2015). Previous studies have demonstrated that α-Syn oligomers could suppress macroautophagy via interaction with Rab1a (Winslow et al. 2010). Furthermore, the enlarged autophagosomes and lysosomes presented in cells overexpressing α-Syn, owing to α-Syn aggregates, resist to degradation leading to a failure of macroautophagy pathway and accumulation of autophagosomes (Tanik et al. 2013). As part of the proteostasis network, autophagy exerts to proteome integrity and principally plays an adaptive or a 'programmed cell survival' role to protect or harm organisms during different situations (Booth et al. 2014). Hence, to determine the role of autophagy in Mn-induced α-Syn oligomerization and neurotoxicity, we applied Rap, which is a promoter of autophagy, and 3-MA, as an inhibitor of autophagy to pretreat α-Syn$^{+/+}$ mice in this study. Our results showed that the pretreatment with Rap (3-MA) had no effects on the brain accumulation of Mn. Moreover, considering to eliminate autophagy dysfunction (overactivation or suppression) to cause adverse effects, we chose a reasonable and effective Rap and 3-MA dosage to pretreat α-Syn$^{+/+}$ mice, which was supported by an increase of LC3-II/I with p62 reduction in Rap control group and an increase of p62 in 3-MA control group, meanwhile, without significant changes of apoptosis and autophagy occurrence. As expected, Rap pretreatment could upregulate autophagy to promote the degradation of Mn-induced α-Syn oligomers and yet further accumulation induced by 3-MA. Additionally, apoptosis also appeared the same change. These results indicated that activation of autophagy could ameliorate Mn-induced α-Syn oligomerization and apoptosis. Taken together, our results further revealed that the α-Syn oligomerization might be

more causative for Mn-induced neurotoxicity than excessive autophagy.

In conclusion, our data demonstrated the neuroprotective role of α-Syn in ameliorating Mn-induced excessive autophagy and neurocytes injury by α-Syn$^{+/+}$ vs. α-Syn$^{-/-}$ mice. Besides, we also revealed the important role of autophagy in the regulation of Mn-induced α-Syn oligomerization and neurocytes injury by Rap or 3-MA pretreatment in vivo. Additional studies are required to verify the detailed mechanism of their interactions in vitro. Hopefully, the neuroprotective role of autophagy in regulating effectively the intracellular homeostasis of α-Syn may act as a potent impetus for neurodegeneration.

Funding This work was supported by the National Natural Science Foundation of China (81773377).

Compliance with Ethical Standards

Ethical Approval Animal treatment and care were in accordance with the National Institutes of Health Guidelines for the Care and Use of Laboratory Animals and approved by the Animal Ethical Committee of China Medical University.

Conflict of Interest The authors declare that they have no conflict of interest.

References

Benskey MJ, Perez RG, Manfredsson FP (2016) The contribution of alpha synuclein to neuronal survival and function—implications for Parkinson's disease. J Neurochem 137:331–359

Booth LA, Tavallai S, Hamed HA, Cruickshanks N, Dent P (2014) The role of cell signalling in the crosstalk between autophagy and apoptosis. Cell Signal 26:549–555

Braak H, Del Tredici K (2017) Neuropathological staging of brain pathology in sporadic Parkinson's disease: separating the wheat from the chaff. J Park Dis 7:S73–s87

Chen P, Chakraborty S, Mukhopadhyay S, Lee E, Paoliello MM, Bowman AB, Aschner M (2015) Manganese homeostasis in the nervous system. J Neurochem 134:601–610

Ciechanover A, Kwon YT (2015) Degradation of misfolded proteins in neurodegenerative diseases: therapeutic targets and strategies. Exp Mol Med 47:e147

Ding L, Wang S, Qu X, Wang J (2016) Tanshinone IIA sensitizes oral squamous cell carcinoma to radiation due to an enhanced autophagy. Environ Toxicol Pharmacol 46:264–269

Gonzalez-Horta A (2015) The interaction of alpha-synuclein with membranes and its implication in Parkinson's disease: a literature review. Nat Prod Commun 10:1775–1778

Harischandra DS, Jin H, Anantharam V, Kanthasamy A, Kanthasamy AG (2015) Alpha-Synuclein protects against manganese neurotoxic insult during the early stages of exposure in a dopaminergic cell model of Parkinson's disease. Toxicol Sci 143:454–468

Horning KJ, Caito SW, Tipps KG, Bowman AB, Aschner M (2015) Manganese is essential for neuronal health. Annu Rev Nutr 35:71–108

Jackson MP, Hewitt EW (2016) Cellular proteostasis: degradation of misfolded proteins by lysosomes. Essays Biochem 60:173–180

Janda E, Lascala A, Carresi C, Parafati M, Aprigliano S, Russo V, Savoia C, Ziviani E, Musolino V, Morani F, Isidoro C, Mollace V (2015) Parkinsonian toxin-induced oxidative stress inhibits basal autophagy in astrocytes via NQO2/quinone oxidoreductase 2: implications for neuroprotection. Autophagy 11:1063–1080

Koga H, Martinez-Vicente M, Arias E, Kaushik S, Sulzer D, Cuervo AM (2011) Constitutive upregulation of chaperone-mediated autophagy in Huntington's disease. J Neurosci 31:18492–18505

Krishna S, Dodd CA, Hekmatyar SK, Filipov NM (2014) Brain deposition and neurotoxicity of manganese in adult mice exposed via the drinking water. Arch Toxicol 88:47–64

Li Y, Jiao Q, Du X, Bi M, Han S, Jiao L, Jiang H (2018) Investigation of behavioral dysfunctions induced by monoamine depletions in a mouse model of Parkinson's disease. Front Cell Neurosci 12:241

Massey AC, Kaushik S, Sovak G, Kiffin R, Cuervo AM (2006) Consequences of the selective blockage of chaperone-mediated autophagy. Proc Natl Acad Sci U S A 103:5805–5810

Matsushita Y, Sakai Y, Shimmura M, Shigeto H, Nishio M, Akamine S, Sanefuji M, Ishizaki Y, Torisu H, Nakabeppu Y, Suzuki A, Takada H, Hara T (2016) Hyperactive mTOR signals in the proopiomelanocortin-expressing hippocampal neurons cause age-dependent epilepsy and premature death in mice. Sci Rep 6:22991

O'Neal SL, Zheng W (2015) Manganese toxicity upon overexposure: a decade in review. Curr Environ Health Rep 2:315–328

Pan J, He L, Li X, Li M, Zhang X, Venesky J, Li Y, Peng Y (2017) Activating autophagy in hippocampal cells alleviates the morphine-induced memory impairment. Mol Neurobiol 54:1710–1724

Peres TV, Parmalee NL, Martinez-Finley EJ, Aschner M (2016) Untangling the manganese-alpha-Synuclein web. Front Neurosci 10:364

Pfalzer AC, Bowman AB (2017) Relationships between essential manganese biology and manganese toxicity in neurological disease. Curr Environ Health Rep 4:223–228

Ravanan P, Srikumar IF, Talwar P (2017) Autophagy: the spotlight for cellular stress responses. Life Sci 188:53–67

Rial D, Castro AA, Machado N, Garcao P, Goncalves FQ, Silva HB, Tome AR, Kofalvi A, Corti O, Raisman-Vozari R, Cunha RA, Prediger RD (2014) Behavioral phenotyping of Parkin-deficient mice: looking for early preclinical features of Parkinson's disease. PLoS One 9:e114216

Tanik SA, Schultheiss CE, Volpicelli-Daley LA, Brunden KR, Lee VM (2013) Lewy body-like alpha-synuclein aggregates resist degradation and impair macroautophagy. J Biol Chem 288:15194–15210

Tetreault P, Dansereau MA, Dore-Savard L, Beaudet N, Sarret P (2011) Weight bearing evaluation in inflammatory, neuropathic and cancer chronic pain in freely moving rats. Physiol Behav 104:495–502

Wang C, Xu B, Ma Z, Liu C, Deng Y, Liu W, Xu ZF (2017a) Inhibition of calpains protects Mn-induced neurotransmitter release disorders in synaptosomes from mice: involvement of SNARE complex and synaptic vesicle fusion. Sci Rep 7:3701

Wang L, Wang J, Yang L, Zhou SM, Guan SY, Yang LK, Shi QX, Zhao MG, Yang Q (2017b) Effect of Praeruptorin C on 3-nitropropionic acid induced Huntington's disease-like symptoms in mice. Biomed Pharmacother 86:81–87

Winslow AR, Chen CW, Corrochano S, Acevedo-Arozena A, Gordon DE, Peden AA, Lichtenberg M, Menzies FM, Ravikumar B, Imarisio S, Brown S, O'Kane CJ, Rubinsztein DC (2010) Alpha-Synuclein impairs macroautophagy: implications for Parkinson's disease. J Cell Biol 190:1023–1037

Wirawan E, Lippens S, Vanden Berghe T, Romagnoli A, Fimia GM, Piacentini M, Vandenabeele P (2012) Beclin1: a role in membrane dynamics and beyond. Autophagy 8:6–17

Wu H, Chen S, Ammar AB, Xu J, Wu Q, Pan K, Zhang J, Hong Y (2015) Crosstalk between macroautophagy and chaperone-mediated autophagy: implications for the treatment of neurological diseases. Mol Neurobiol 52:1284–1296

Xilouri M, Brekk OR, Stefanis L (2016) Autophagy and alpha-synuclein: relevance to Parkinson's disease and related Synucleopathies. Mov Disord 31:178–192

Xu B, Jin CH, Deng Y, Liu W, Yang TY, Feng S, Xu ZF (2014a) Alpha-synuclein oligomerization in manganese-induced nerve cell injury in brain slices: a role of NO-mediated S-nitrosylation of protein disulfide isomerase. Mol Neurobiol 50:1098–1110

Xu B, Wang F, Wu SW, Deng Y, Liu W, Feng S, Yang TY, Xu ZF (2014b) Alpha-synuclein is involved in manganese-induced ER stress via PERK signal pathway in organotypic brain slice cultures. Mol Neurobiol 49:399–412

Xu B, Liu W, Deng Y, Yang TY, Feng S, Xu ZF (2015) Inhibition of calpain prevents manganese-induced cell injury and alpha-synuclein oligomerization in organotypic brain slice cultures. PLoS One 10: e0119205

Yasuhara K, Ohno Y, Kojima A, Uehara K, Beppu M, Sugiura T, Fujimoto M, Nakai A, Ohira Y, Yoshioka T, Goto K (2011) Absence of heat shock transcription factor 1 retards the regrowth of atrophied soleus muscle in mice. J Appl Physiol (1985) 111: 1142–1149

Yuan Z, Ying XP, Zhong WJ, Tian SM, Wang Y, Jia YR, Chen W, Fu JL, Zhao P, Zhou ZC (2016) Autophagy attenuates MnCl2-induced apoptosis in human bronchial epithelial cells. Biomed Environ Sci 29: 494–504

Zhang J, Cao R, Cai T, Aschner M, Zhao F, Yao T, Chen Y, Cao Z, Luo W, Chen J (2013) The role of autophagy dysregulation in manganese-induced dopaminergic neurodegeneration. Neurotox Res 24:478–490

Zhang Z, Miah M, Culbreth M, Aschner M (2016) Autophagy in neurodegenerative diseases and metal neurotoxicity. Neurochem Res 41: 409–422